JOURNAL OF VIROLOGY, Feb. 1997, p. 1386–1396 Vol. 71, No. 2
0022-538X/97/$04.00+0

S-Phase-Dependent Cell Cycle Disturbances Caused by Aleutian Mink Disease Parvovirus

MARTIN B. OLEKSIEWICZ[1] AND SOREN ALEXANDERSEN[2]*

Laboratory for Veterinary Pathology, Department of Pharmacology and Pathobiology, Royal Veterinary and Agricultural University, DK-1870 Frederiksberg C,[1] and Danish Veterinary Institute for Virus Research, DK-4771 Kalvehave,[2] Denmark

Received 1 August 1996/Accepted 28 October 1996

We examined replication of the autonomous parvovirus Aleutian mink disease parvovirus (ADV) in relation to cell cycle progression of permissive Crandell feline kidney (CRFK) cells. Flow cytometric analysis showed that ADV caused a composite, binary pattern of cell cycle arrest. ADV-induced cell cycle arrest occurred exclusively in cells containing de novo-synthesized viral nonstructural (NS) proteins. Production of ADV NS proteins, indicative of ADV replication, was triggered during S-phase traverse. The NS^+ cells that were generated during later parts of S phase did not undergo cytokinesis and formed a distinct population, termed population A. Formation of population A was not prevented by VM-26, indicating that these cells were arrested in late S or G_2 phase. Cells in population A continued to support high-level ADV DNA replication and production of infectious virus after the normal S phase had ceased. A second, postmitotic, NS^+ population (termed population B) arose in G_0/G_1, downstream of population A. Population B cells were unable to traverse S phase but did exhibit low-level DNA synthesis. Since the nature of this DNA synthesis was not examined, we cannot at present differentiate between G_1 and early S arrest in population B. Cells that became NS^+ during S phase entered population A, whereas population B cells apparently remained NS^- during S phase and expressed high NS levels postmitosis in G_0/G_1. This suggested that population B resulted from leakage of cells with subthreshold levels of ADV products through the late S/G_2 block and, consequently, that the binary pattern of ADV-induced cell cycle arrest may be governed merely by viral replication levels within a single S phase. Flow cytometric analysis of propidium iodide fluorescence and bromodeoxyuridine uptake showed that population A cells sustained significantly higher levels of DNA replication than population B cells during the ADV-induced cell cycle arrest. Therefore, the type of ADV-induced cell cycle arrest was not trivial and could have implications for subsequent viral replication in the target cell.

Aleutian mink disease parvovirus (ADV) causes a slow, chronic infection termed Aleutian disease in adult mink. Aleutian disease is characterized by viral persistence, hypergammaglobulinemia, plasmacytosis, increased relative levels of circulating $CD8^+$ lymphocytes, and immune complex-mediated tissue injury such as glomerulonephritis and arteriitis (1, 37; for reviews, see references 2 and 12).

In Aleutian disease, restricted ADV replication occurs in lymphoid tissue (5). In contrast, in newborn, seronegative mink kits, ADV causes acute pneumonia due to high-level cytopathic replication in type II pneumocytes (3, 7, 55). This suggests that downregulation of viral replication to semipermissive levels, which fail to reach cytotoxic thresholds, may be important in chronic ADV infection (2, 8, 19, 45, 53). Consequently, factors affecting ADV replication on the cellular level are of interest in elucidating the pathogenesis of Aleutian disease.

Generally, replication of autonomous parvoviruses requires cell proliferation (20, 47). Cellular S-phase-associated factors are required for initial transformation of the single-stranded DNA genome to a transcriptionally active double-stranded template, as well as for further viral DNA replication (for a recent review, see reference 22). Also, differentiation and transformation may modify the ability of cells to support parvovirus replication (48, 54). In turn, parvoviruses exert cytostatic and cytotoxic effects, which are mediated mainly through the major viral nonstructural (NS) protein NS1 (17, 40, 54).

The proliferative status of the target cell is thus assumed to be of major importance for replication of ADV in vivo, but the fundamental relationship between ADV replication and cell proliferation has not been examined. Therefore, we investigated ADV replication in relation to cell cycle progression of permissive Crandell feline kidney (CRFK) cells.

MATERIALS AND METHODS

Cell cultures and virus stock. The Gorham-Lund isolate (2, 7) of ADV was obtained from the Danish Fur Breeders Laboratory (Glostrup, Denmark). An ADV stock was prepared by freeze-thawing infected CRFK cells (14). A mock inoculum was similarly prepared from uninfected CRFK cultures.

CRFK cultures were maintained at 31.8°C in Dulbecco's modified Eagle's medium supplemented with 5% fetal calf serum (FCS) (Gibco-BRL, Roskilde, Denmark), 2 mM L-glutamine (Gibco-BRL), 100 U of penicillin G (Sigma, Bie & Berntsen, Rodovre, Denmark) per ml, and 100 μg of streptomycin sulfate (Sigma) per ml. Asynchronous CRFK cultures at 31.8°C were infected with ADV or the mock inoculum at the multiplicity of infection (MOI) indicated in the figure legends (14). After 1 h, the cultures were washed once and refed with fresh, prewarmed medium.

ADV was titrated on CRFK cells at 31.8°C (14). Briefly, CRFK cultures infected with serial dilutions of freeze-thawed cell lysate or cell supernatant were harvested at 3 days postinfection. The percentage of ADV-infected cells was determined by flow cytometric analysis of fixed-cell suspensions that were stained with anti-NS rabbit serum (see below), and the content of infectious ADV was calculated as fluorescence-forming units (FFU) per milliliter.

The CRFK cell stocks and ADV virus stocks used for these experiments were confirmed to be free of mycoplasma contamination by standard microbiological culturing methods and a PCR-based test kit.

Synchronization of CRFK cells. CRFK cultures were synchronized in early S phase by using a modification of existing protocols (28).

First, cells were synchronized in G_0 by maintaining confluent CRFK cultures at 37°C in medium with 5% FCS for 2 to 4 days and with 0% FCS for the last

* Corresponding author. Mailing address: Danish Veterinary Institute for Virus Research, DK-4771 Kalvehave, Denmark. Phone: (45) 5581 4523. Fax: (45) 5581 1766. E-mail: SA@SVIV.LFM.DK.

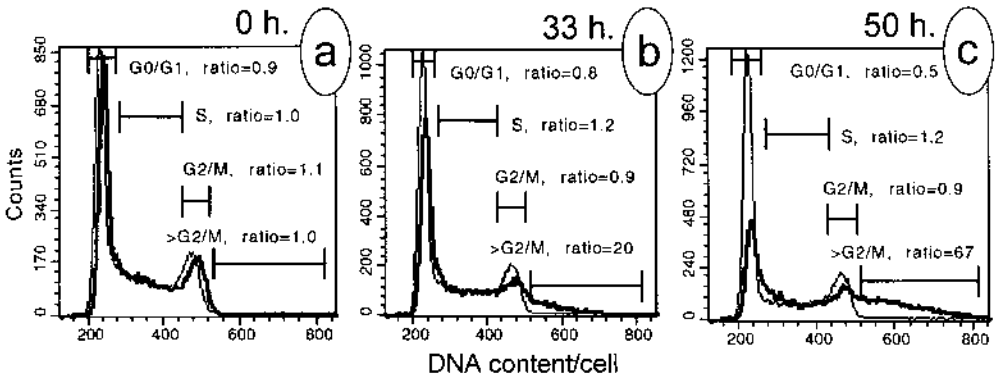

FIG. 1. ADV-induced cell cycle disturbances in asynchronous cultures. CRFK cultures in exponential growth were infected with ADV at 10 FFU/cell or mock infected. Cultures were harvested at 0, 33, and 50 h postinfection. Cell cycle distributions of ADV- and mock-infected cultures were compared by flow cytometric analysis of PI-stained cell suspensions. Overlaid DNA histograms of ADV (thick lines)- and mock (thin lines)-infected cultures at the indicated times postinfection are shown. In each overlaid plot, the two histograms are shown on the same scale and contain the same number of events, so that peak heights can be compared. The markers indicate the positions of the G_0/G_1, S, and G_2/M phases, as well as the $>G_2$/M events unique to ADV-infected cultures. The fraction of ADV-infected cells contained in each marker was divided by the fraction of mock-infected cells contained in each marker, to yield the indicated ratios. Ratios of below 1 indicate underrepresentation of a cell cycle phase in ADV-infected cultures, whereas ratios of above 1 indicate that ADV-infected cells arrest in the given cell cycle phase.

24 h. The cells were then released from the G_0 block by trypsinization (0.05% trypsin in EDTA [both from Gibco-BRL]) and reseeding at subconfluent densities (5×10^5 to 8×10^5 cells in 60-mm-diameter dishes [Costar, Meda, Soborg, Denmark]) in medium containing 10% FCS and 2 mM hydroxyurea (HU) (Sigma). The dishes were incubated for 1 h at 37°C to allow the cells to adhere. Mock inoculum or ADV stock was added at the MOI indicated in the figure legends, and the cultures were incubated for a further 24 h at 37°C. During the incubation in HU, cultures traversed G_1, and they became arrested in very early S phase. After a total of 25 h at 37°C, cells were released from the HU block by being washed once with prewarmed medium and were incubated at 31.8°C (a more permissive temperature for ADV replication [11, 14, 29]) in fresh, prewarmed medium. Cultures intended for virus titration received an additional wash with trypsin-EDTA (30 s, room temperature) to remove noninternalized virus. The time of release from the HU block is always 0 h below.

In some experiments, synchronized cultures were treated with the following drugs or enzymes. Colcemide (Karyo-Max; Gibco-BRL), which causes metaphase arrest due to disruption of microtubule assembly, was used at 50 ng/ml. VM-26 (Vumon infusion concentrate, a generous gift of J. Stone, Bristol-Myers Squibb, Lyngby, Denmark), which causes G_2 arrest due to inhibition of topoisomerase II, was used at 0.5 μg/ml (52). The base in which these drugs were formulated from the manufacturer did not in itself cause cell cycle arrest of CRFK cells. *Clostridium perfringens* neuraminidase (0.025 U/ml) (type X; Sigma) was used to prevent reinfection (21). When neuraminidase was added to CRFK cultures before the ADV inoculum, a 7- to 10-fold reduction in the number of infected cells resulted, showing that neuraminidase was effective in preventing ADV infection (not shown).

Cell counts, viability, and immunofluorescence analysis. Cultures were harvested by trypsinization. Pooled loose and adherent cells were counted in a Neubauer hemacytometer. Cells in triplicate cultures were counted at each time point, with counts typically deviating less than 10%. Cell viability was determined by trypan blue exclusion.

For immunofluorescence analysis of mitotic cells, cells were swollen for 10 min in distilled water on ice and fixed in 70% ethanol. Cytospins of ethanol-fixed cell suspensions were stained with the anti-NS serum and fluorescein isothiocyanate (FITC)-conjugated secondary antibody described below, essentially as described previously (38). Cytospins were mounted in buffered glycerol containing 25 mg of 1,4-diaza-bicyclo-[2.2.2]octane (DABCO) (Sigma) per ml and 1 μg of 4′,6-diamidino-2-phenylindole (DAPI) (Sigma) per ml prior to examination by fluorescence microscopy.

Antibodies. Rabbit immune serum raised against baculovirus-produced ADV NS1 protein (kindly provided by J. Christensen) was used at a 1:500 dilution. By flow cytometric analysis (see below), this serum detected CRFK cells transiently transfected with either NS1 or NS2 expression plasmids (not shown), due to the common amino terminus in the two NS proteins (4, 18). FITC-conjugated swine anti-rabbit immunoglobulin (DAKO, Glostrup, Denmark) was used as a secondary antibody.

A monoclonal antibody (MAb) against 5-bromo-2′-deoxyuridine (BrdU) (Bu 20; DAKO) was used at a 1:5 dilution. FITC-conjugated rabbit anti-mouse immunoglobulin (DAKO) was used as a secondary antibody.

Flow cytometric analysis. CRFK cultures were harvested by trypsinization. Where indicated, cultures were labelled for 2 h immediately prior to harvest with 10 μM BrdU (Sigma). Pooled loose and adherent cells were pelleted, resuspended in cold (4°C) phosphate-buffered saline, and fixed by adding 10 volumes of cold 70% ethanol. Fixed-cell suspensions were stored at −20°C.

Ethanol-fixed cells were double stained for ADV NS proteins and total DNA content, essentially as described previously (16). Briefly, ethanol-fixed cells were immunostained for NS proteins with the serum and secondary FITC conjugate described above and resuspended in a propidium iodide (PI) solution (50 μg of PI [Sigma] per ml, 2 mg of DNase-free RNaseI [Pharmacia, Allerod, Denmark] per ml, 1.12% trisodium citrate [pH 7.4]) at 1×10^6 to 2×10^6 cells/ml. Samples were incubated for 20 min in the dark at room temperature before flow cytometric analysis.

Double staining for BrdU and total DNA content was done as described previously (27). Briefly, ethanol-fixed cells were digested in 0.16 mg of pepsin per ml–1.6 M HCl for 30 min at 37°C. The digestion yields a suspension of cell nuclei, in which the BrdU epitope is accessible to MAb staining. Nuclei were immunostained for BrdU with the MAb and secondary FITC conjugate described above and resuspended in PI solution prior to flow cytometric analysis.

Samples were analyzed on a FACSCALIBUR flow cytometer (Becton-Dickinson, Brondby, Denmark). Statistical analysis was done with Cell-Quest software (Becton-Dickinson).

[*methyl*-^{3}H]thymidine labelling. Synchronized cultures were labelled with 10 μCi of [*methyl*-^{3}H]thymidine (1 mCi/ml, 82 Ci/mmol; Amersham, Birkerod, Denmark) per ml for 2 h immediately prior to harvest by trypsinization. Pooled loose and adherent cells were washed once in phosphate-buffered saline and resuspended in TE (10 mM Tris, 1 mM EDTA, pH 7.5). Crude sodium dodecyl sulfate (SDS) lysates were made by adding SDS (Gibco-BRL) to 0.1% and proteinase K (Gibco-BRL) to 400 μg/ml and incubating samples for 2 h at 60°C.

To quantify total [^{3}H]thymidine incorporation, the crude SDS lysate was mixed with 20 volumes of salmon sperm DNA (250 μg/ml) in distilled water and deposited on Whatman GF/C glass fiber filters. The filters were washed twice with ice-cold HCl-pyrophosphate solution and once with 96% ethanol and placed in Opti-Phase Hi-Safe II scintillant (Wallac, Allerod, Denmark) prior to liquid scintillation spectrometry.

To examine [^{3}H]thymidine incorporation in viral and cellular DNAs separately, SDS lysates were electrophoresed in 1% agarose gels. Prior to submerging of gels in running buffer, the wells were plugged with 65°C warm agarose. The gels were fixed in isopropanol-H_2O-acetic acid (25:65:10), soaked for 2 h in Amplify fluorographic reagent (Amersham), dried, and exposed to Kodak X-AR film for 0.5 to 9 days at −80°C.

Southern blot analysis. Synchronized CRFK cultures were harvested at various times postrelease, and crude SDS lysates were prepared as described above. Lysates were electrophoresed in 1% agarose gels. Southern blotting and probing of blots with a ^{32}P-labelled ADV plus-sense riboprobe (which detects all ADV DNA species) were done as previously described (3, 15).

RESULTS

ADV causes cell cycle disturbances in permissive cells. We initially examined the effect of ADV infection on cell cycle progression in asynchronous cultures. We found that the main effect of ADV infection was a reduction in G_0/G_1-phase cells and a simultaneous increase in cells with more than G_2/M ($>G_2$/M) DNA contents (Fig. 1c). At 50 h postinfection, ADV-infected cultures contained 2 times fewer G_0/G_1-phase cells

and 67 times more $>G_2$/M-phase cells than did mock-infected cultures (Fig. 1c). ADV did not induce formation of multinucleate cells, and the $>G_2$/M events in ADV-infected cultures were also observed when isolated nuclei were analyzed (see Fig. 5b). Therefore, ADV infection caused cells to accumulate abnormally high nuclear DNA contents.

ADV-induced cell cycle disturbances were associated with inhibition of cell proliferation (as estimated by cell counts), and we did not observe any mitogenic effect of ADV infection in cultures made quiescent by confluency or serum deprivation (not shown). This suggested that the reduction in G_0/G_1-phase cells (Fig. 1c) was a result of the accumulation of noncycling $>G_2$/M-phase cells, as opposed to the accumulation of $>G_2$/M-phase cells being an effect of mitogenic stimulation of G_0/G_1-phase cells. We then examined the relationship between viral replication and cell cycle arrest in greater detail in synchronized cultures.

ADV-induced cell cycle disturbances are S-phase dependent and composite and require the presence of NS proteins. A double-block protocol utilizing combined topoinhibition and serum deprivation, followed by HU exposure, was used to generate CRFK cultures synchronized in early S phase. At 0 h, more than 90% of the cells had G_0/G_1 DNA contents. Following release from the HU block, mock-infected cells traversed a synchronous S phase of 12 to 14 h, underwent mitosis from 16 to 21 h, and had returned to G_1 by 25 h (Fig. 2a). In contrast, a significant proportion of cells in ADV-infected cultures were seen to continue DNA synthesis from 12 to 25 h, leading to accumulation of $>G_2$/M DNA (Fig. 2b). At 25 h, 89% of mock-infected cells were in G_0/G_1 (Fig. 2d). In contrast, only 56% of cells in ADV-infected cultures were in G_0/G_1 (Fig. 2e). Thus, the cell cycle disturbances observed in asynchronous cultures were recapitulated in synchronized cultures. When viewed in a cause-effect perspective, S-phase transit triggered accumulation of $>G_2$/M-phase cells, and the $>G_2$/M-phase cells failed to undergo cytokinesis, causing a reduced percentage of G_0/G_1-phase cells at 25 h. Importantly, viabilities judged by trypan blue exclusion were similar (>90%) in ADV- and mock-infected cultures at 25 h, making it unlikely that ADV-induced cell lysis contributed to the reduction in G_0/G_1-phase cells.

We related the ADV-induced cell cycle disturbances to viral replication by bivariate flow cytometric analysis of ADV NS protein content versus total DNA content (Fig. 2f to m). Anti-NS staining was used because NS proteins are required for parvovirus replication and are expressed early in the viral life cycle (22, 43).

In ADV-infected cultures, the percentage of NS^+ cells increased as cultures progressed through S phase, and it reached 40% at 12 h, corresponding to very late S phase (Fig. 2f to j). Similar results were obtained with cultures parasynchronized by serum deprivation only, indicating that ADV gene expression depended on S-phase entry per se and not on release from the HU block (not shown).

We observed that the background NS staining of NS^- cells in ADV-infected cultures increased over time and became 2.4 times higher than that in mock-infected cultures at 25 h (Fig. 2l and m). When ADV-infected and mock-infected cells were mixed prior to ethanol fixation and staining, the mock-infected cells exhibited a strongly increased background staining (not shown). This suggested that the increase in background staining of NS^- cells in ADV-infected cultures was due to passive transfer of NS proteins from NS^+ to NS^- cells during ethanol fixation or staining and was not caused by low-level NS protein synthesis in NS^- cells.

Bivariate analysis showed that $>G_2$/M DNA synthesis from 12 to 25 h was restricted to NS^+ cells. The NS^+ population which accumulated $>G_2$/M DNA formed during S phase and was termed population A (Fig. 2f to j). Population A was recruited mainly from mid- and late-S-phase cells (Fig. 2h to j), whereas only few NS^+ cells appeared in early S phase (Fig. 2g and h). Assuming that all of the NS^+ cells generated during S phase (40%) (Fig. 2j, population A) did not undergo cytokinesis and accumulated $>G_2$/M DNA, while NS^- cells (60%) (Fig. 2j) underwent cytokinesis, the expected percentage of $>G_2$/M-phase cells postmitosis would be $40/(40 + 2 \times 60) = 25\%$. This value corresponded well to the observed 28% $>G_2$/M-phase cells (Fig. 2e). Thus, comparison of the sizes of population A before and after mitosis strongly suggested that the majority, if not all, of the NS^+ cells generated during S phase (Fig. 2j, population A) went on to synthesize $>G_2$/M DNA and did not undergo cytokinesis. The average PI fluorescence of population A continued to increase from 12 to 25 h (Fig. 2j to l). Thus, although population A cells did not undergo cytokinesis and were rendered noncycling, they remained metabolically active and exhibited high levels of cumulative DNA synthesis from 12 to 25 h. In contrast, NS^- cells in infected cultures ceased DNA synthesis at 12 to 14 h and exhibited unhindered progress through G_2 and M into G_0/G_1, indistinguishable from the case for mock-infected cells (compare Fig. 2a and c).

Interestingly, a second population of NS^+ cells (termed population B) (Fig. 2k) was revealed by the bivariate analysis. At steady-state conditions, population B contained a minority (30 to 45%) of the NS^+ cells. In contrast to population A, population B did not form during S phase (Fig. 2j). Instead, population B arose in G_0/G_1, in exact synchrony with mitosis of NS^- cells from 16 to 21 h (Fig. 2k). Therefore, formation of population B required S-, G_2-, and M-phase traverse by infected cells.

A trypsin-EDTA wash followed by neuraminidase treatment immediately after release from the HU block had no effect on the appearance of population B (not shown). This indicated that the difference between population A and B cells was not one of virus internalization and also that reinfection did not play a role. Populations A and B were also observed with MAbs and polyclonal antibodies against capsid proteins (not shown).

As mentioned above, our results showed that the NS^+ cells generated during S phase (Fig. 2j, population A) did not undergo cytokinesis. Thus, the appearance of population B in turn suggested that some infected cells remained NS^- during S-phase traverse and started significant NS protein production postmitosis, in G_0/G_1 (Fig. 2k). To examine this possibility, mitotic cells were examined for NS protein content. In ADV-infected cultures, cells with undisturbed mitotic morphology contained either no NS proteins, or, rarely, low NS protein levels (Fig. 3a, arrowhead [compare to neighboring nucleus without NS protein, indicated by arrow in Fig. 3b]). High NS levels were found in interphase nuclei (Fig. 3a, arrows), in cells with disintegrating nuclei (Fig. 3b, arrowhead), and, rarely, in cells with apparently severely perturbed mitotic chromatin (not shown). We described the intracellular localization of ADV products in more detail in a recent study (33). The absence, or low-level presence, of NS proteins in cells with undisturbed mitotic chromatin (Fig. 3a, arrowhead) was in agreement with the flow cytometric findings described above, i.e., that population B resulted from mitosis of infected cells that had remained NS^- during S-phase traverse. Taken together, our results indicated that the level of ADV replication reached through S phase might influence whether cells underwent mitosis and

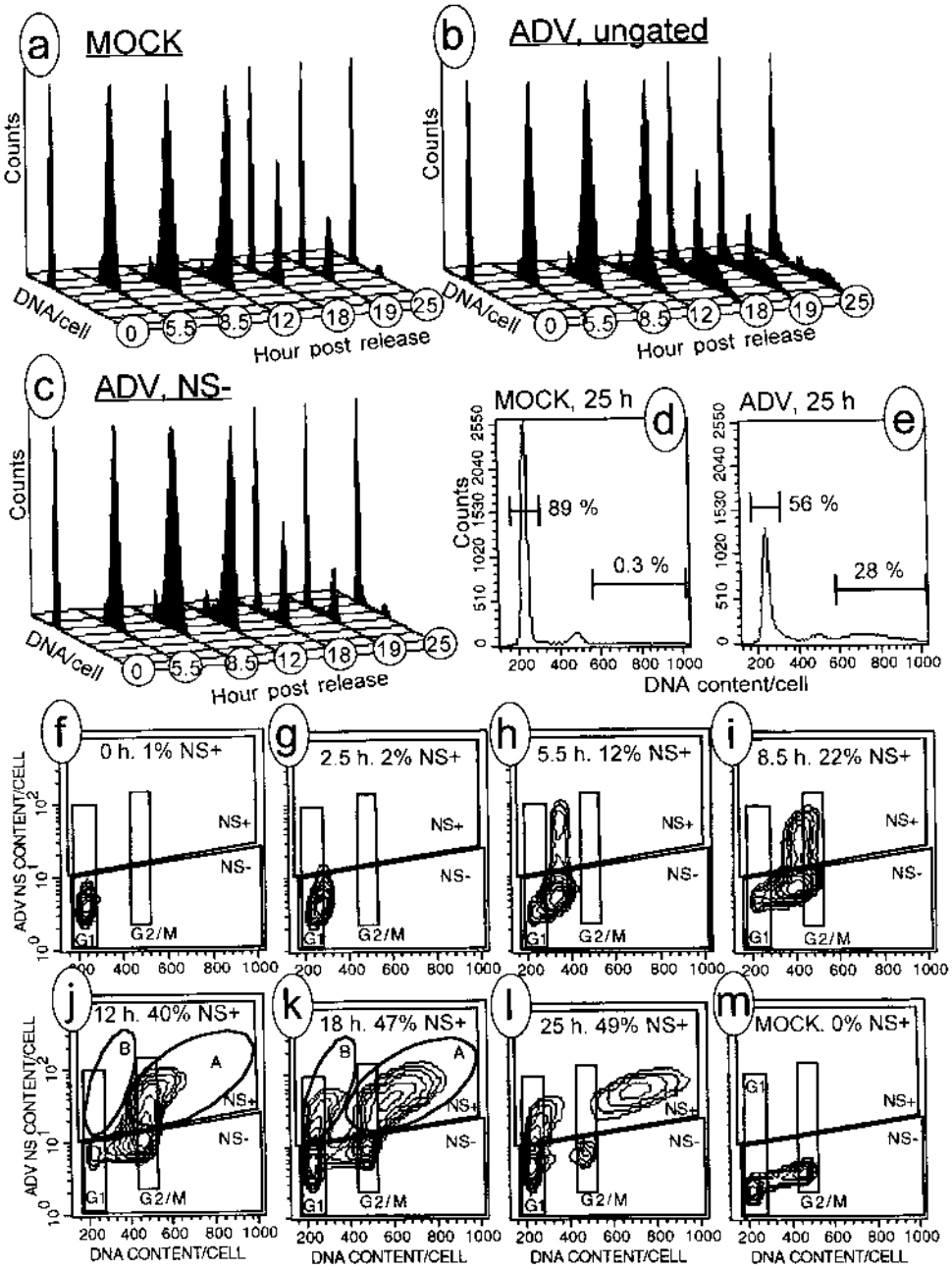

FIG. 2. Passage of ADV-infected cells through the first S, G_2, and M phases. Synchronized cultures were infected with ADV at 10 FFU/cell or mock infected. Cell suspensions double stained for ADV NS proteins and total DNA content were analyzed by flow cytometry. (a to c) DNA distributions (PI fluorescence) of cultures harvested at the indicated time postrelease. Histograms are scaled individually, so peak positions but not peak heights can be compared. Results for mock-infected cultures (ungated) (a), ADV-infected cultures (ungated) (b), and gated NS^- cells in ADV-infected cultures (c) are shown (the NS^- gate is shown in panels f to m). (d and e) DNA distributions of mock (d)- and ADV (e)-infected cultures at 25 h postrelease, after passage through S, G_2, and M. Histograms are shown on same scale and contain same number of events. The percentages of cells in G_0/G_1 (left markers) and $>G_2/M$ (right markers) are indicated. (f to m) Bivariate analysis of ADV NS protein content (FITC fluorescence, logarithmic *y* axis) versus total DNA content (PI fluorescence, linear *x* axis). Contours show 65% differences in event number (logarithmic spacing) after a 1.5% background subtraction. The regions indicating positions of G_1-phase, G_2/M-phase, NS^+ and NS^- cells have same positions in all plots. Note that whereas the cell cycle position of NS^- cells is reflected by DNA content, the cell cycle position of NS^+ cells is open to interpretation (see text). Positions of populations A and B of NS^+ cells are indicated by oval regions in j and k. In each plot the time after release and the percentage of NS^+ cells are indicated.

thus might determine the distribution of infected cells into populations A and B.

Population B cells do not traverse S phase. Since population A cells were rendered noncycling as a consequence of ADV infection, the proliferative capacity of population B cells was of interest. We examined the ability of population B cells to cycle in stathmokinetic-type experiments (23) (Fig. 4). An MOI five-fold lower than that for the experiment shown in Fig. 2 was used, in order to improve culture viability during the extended experimental period. Colcemide was added to synchronized cultures at 26 h. At this time, the first synchronous mitosis had just occurred (Fig. 2a). Consequently, the majority of NS^-

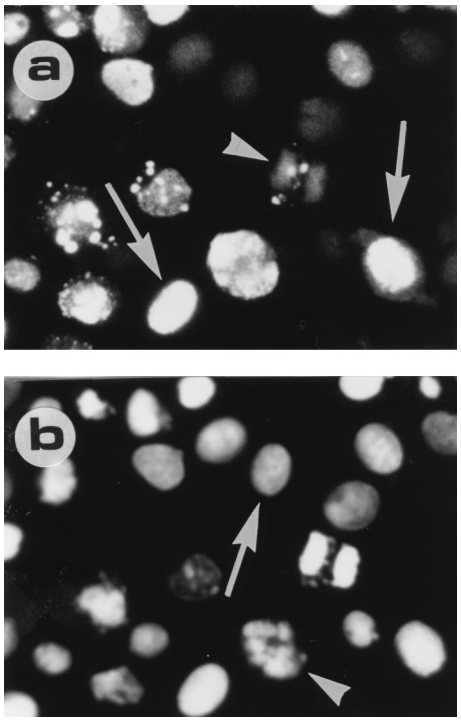

FIG. 3. ADV infection in mitotic cells. ADV-infected, synchronized cells were harvested at 18 h postrelease. Cells were immunostained for ADV NS proteins and counterstained with DAPI. Magnification, ×400. (a) FITC fluorescence (NS protein). A mitotic cell containing NS protein (arrowhead) and interphase nuclei containing NS protein (arrows) are indicated. (b) DAPI fluorescence of the cells shown in panel a. A nucleus without NS protein (arrow) and a disintegrating nucleus in a cell containing NS protein (arrowhead) are indicated.

(Fig. 4e, thin line) and mock-infected (Fig. 4h) cells were in G_0/G_1, and population B had formed (Fig. 4e, thick line, M2). No new G_0/G_1-phase cells formed in colcemide-blocked cultures, because colcemide prevented mitosis in CRFK cells (Fig. 4j). No new population B cells formed in colcemide-blocked cultures, because formation of population B required M-phase traverse (discussed above), and colcemide treatment abolished the formation of population B (see Fig. 7b). Consequently, we could compare the abilities of the following cell populations to traverse S phase: (i) population B cells (Fig. 4e to g, thick lines, markers M2), (ii) NS^- G_1-phase cells from the same infected cultures (Fig. 4e to g, thin lines, markers M2), and (iii) mock-infected G_1-phase cells from parallel cultures (Fig. 4h to j).

Mock-infected cultures entered the second S phase in a parasynchronous fashion from 26 to 50 h after release from the HU block. At 74 h, the majority of mock-infected cells had traversed S phase and encountered the colcemide block (Fig. 4h to j). NS^- cells in infected cultures exhibited unhindered S-phase traverse identical to that of mock-infected cells (Fig. 4e to g, thin lines). A four- to sevenfold reduction in G_0/G_1-phase cells had occurred at 74 h for both NS^- and mock-infected cells (Fig. 4k and l, solid symbols). In contrast, no reduction in the size of population B was observed (Fig. 4k, l, and m, solid symbols). Therefore, cells in population B were inhibited from traversing S phase and were in effect noncycling.

Population A increased in size during the colcemide block (Fig. 4m, open symbols), which required an explanation. The increase in population A did not derive from S-phase traverse of existing population B cells, as discussed above, but instead resulted from the appearance of new NS^+ cells, because the increase in population A (34% − 14% = 21%) (Fig. 4m) corresponded to the increase in NS^+ cells (53% − 33% = 20%) (Fig. 4n). The numbers in these and subsequent calculations are derived by comparing the 26- and 75-h values in Fig. 4k to n.

The new NS^+ cells in population A were recruited from NS^- cells as NS^- cells traversed S phase, by the following argument. For NS^- cells (Fig. 4l), the reduction in G_1-phase cells (58% − 8% = 50%) was larger than the increase in G_2/M-phase cells (28% − 5% = 23%). Therefore, 27% (50% − 23%) of the cells were lost from the NS^- population during S-phase traverse. This loss from the NS^- population during the 48-h colcemide block corresponded well to the gain of 20 to 21% new NS^+ cells in population A during the same period. Therefore, cells moved from the NS^- population into population A during the second S phase, in effect recapitulating the events in the first S phase (Fig. 2f to j).

In estimating the loss or gain from a given cell population based on the percentage of total cells present that the population constitutes (as was done in the calculations described above), the presence of a constant total cell number throughout the experiment was assumed. A modest reduction in cell numbers (15 to 20%) was in fact observed during the 48-h colcemide block (Fig. 4o). The reduction was similar in mock- and ADV-infected cultures, indicating that it might be caused chiefly by colcemide cytotoxicity. Although this physical loss of cells introduced an unknown error in the estimates of cell movements, this error was apparently small enough for the calculations described above to show good concordance.

Cell cycle arrest in populations A and B is associated with different amounts of cumulative DNA synthesis. Although population B cells did not traverse S phase, they nevertheless exhibited a gradual increase in PI fluorescence over time, to 25 to 30% above G_0/G_1 levels. In contrast, population A cells exhibited PI fluorescence of 40 to 50% above G_2/M levels (not shown in detail, but this difference between populations A and B is apparent in Fig. 2k, 4g, and 7a). This suggested that population A cells sustained approximately threefold (2 × 40/25)-higher levels of cumulative DNA synthesis than population B cells during the ADV-induced cell cycle arrest.

We confirmed the presence of DNA synthesis in populations A and B by BrdU labelling (Fig. 5). Fifty-nine percent of cells in ADV-infected cultures (Fig. 5b) but only 12% of cells in mock-infected cultures (Fig. 5e) were $BrdU^+$ at 20 h (i.e., after completion of the first synchronous S phase [Fig. 2a]). No $BrdU^+$ cells were seen in cultures not labelled with BrdU (Fig. 5c and f). Also, BrdU incorporation was inhibited by HU and aphidicolin (not shown), indicating that $BrdU^+$ cells had incorporated BrdU as a result of DNA synthesis. The surplus of 47% (59% − 12%) for $BrdU^+$ cells in ADV-infected cultures corresponded to the percentage of NS^+ cells (44% [Fig. 5a]). This indicated that in ADV-infected cultures, all NS^+ cells were $BrdU^+$ at this time.

The $BrdU^+$ cells in ADV-infected cultures were distributed in two populations (Fig. 5b, R6 and R5) that were similar to populations A and B of NS^+ cells (Fig. 5a, R2 and R1, respectively). In ADV-infected cultures, regions R6 and R5 contained four- to fivefold more $BrdU^+$ cells than the expected levels of NS^- S-phase cells (Fig. 5b and e, compare R5 and R6). Taken together, these findings suggested that BrdU uptake, indicative of DNA synthesis, occurred in population A as well as population B of NS^+ cells. Similar results were obtained in other experiments when colcemide was added to cultures immediately prior to BrdU labelling from 23 to 25 h, confirming that $BrdU^+$ cells in region R5 in ADV-infected cultures (Fig. 5b) had incorporated BrdU after mitosis, that is, after arrival in population B (not shown).

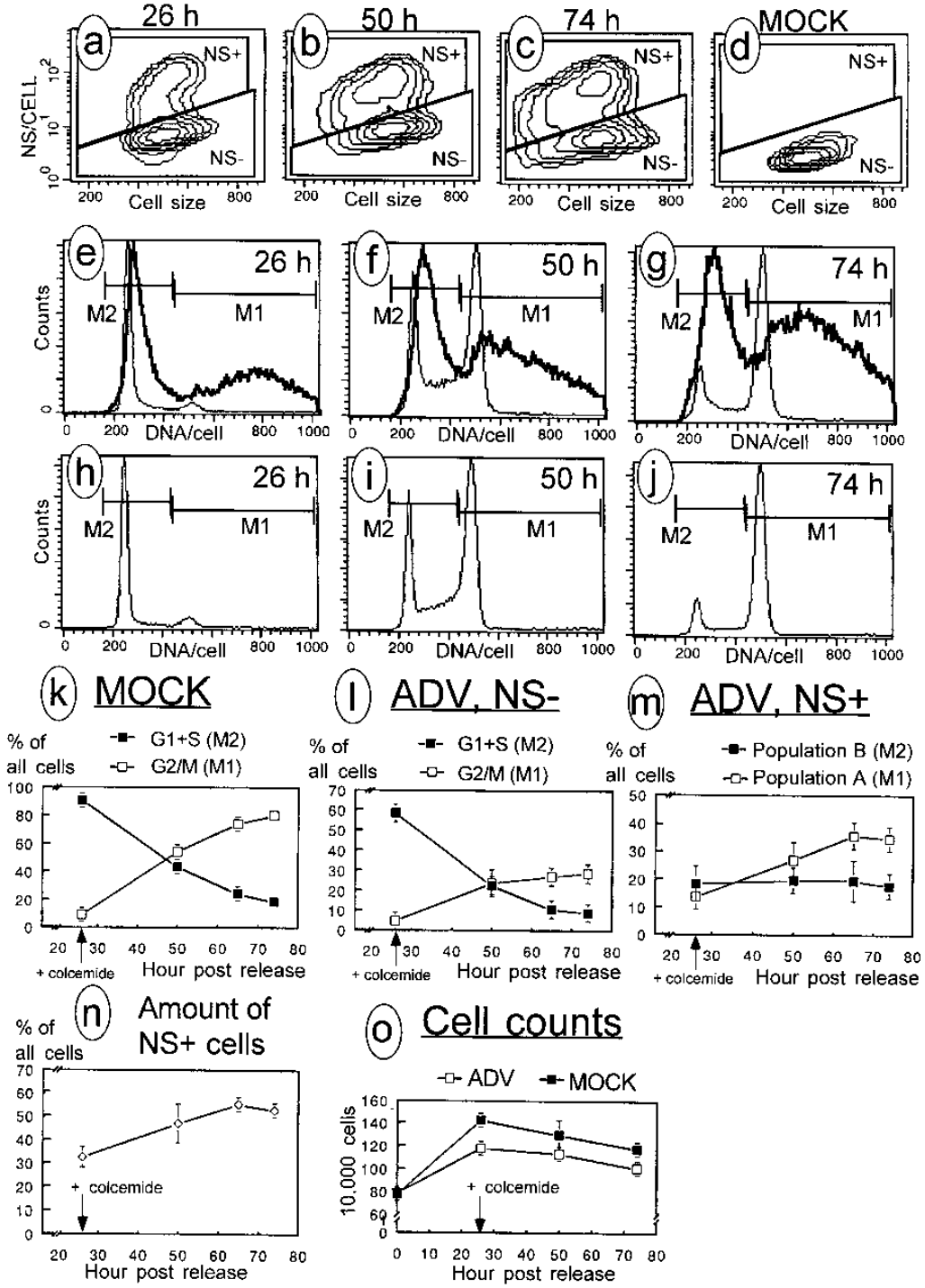

FIG. 4. Movement of ADV-infected cells through the second S phase. Synchronized cultures were infected with ADV at 2 FFU/cell or mock infected. Colcemide (50 ng/ml) was added to all cultures at 26 h postrelease from HU. Cell suspensions double stained for ADV NS proteins and total DNA content were analyzed by flow cytometry. Duplicate cultures were harvested at each time point. In panels a to j, plots from flow cytometric analysis of a single representative culture at the indicated time after release from the HU block are shown. Plots are not shown for the 65-h time point, data from which appears in some of the graphs. Ninety percent confidence intervals were calculated by using Student's *t* distribution. (a to d) Contour plots showing forward light scatter (cell size) on the *x* axis and FITC fluorescence (ADV NS content) on the *y* axis for ADV (a to c)- and mock (d)-infected cultures. The NS^+ and NS^- regions shown were identical for all samples. Less than 0.1% of mock-infected cells were in the NS^+ region. (e to g) Overlaid DNA histograms of NS^+ (thick lines) and NS^- (thin lines) cells from the contour plots in panels a to c, respectively. Populations A and B of NS^+ cells are indicated by markers M1 and M2, respectively. The positions of markers M1 and M2 were identical in these and all subsequent plots. Overlaid histograms were scaled individually (scale not shown). (h to j) DNA histograms of cells from mock-infected cultures. Marker M1 contains G_2/M-phase cells; marker M2 contains G_1 and S (G_1+S)-phase cells. (k to m) Quantification of histogram data for mock-infected cells (k), NS^- cells from ADV-infected cultures (l), and NS^+ cells from the same ADV-infected cultures (m). Cells contained by markers M1 and M2 (shown in panels e to j) are expressed as the percentage of all (ungated) cells in the culture. Each point (except the 74-h point for mock-infected cells) represents the mean of duplicate determinations. Bars indicate 90% confidence intervals. (n) Cells in the NS^+ region (shown in panels a to c) in ADV-infected cultures expressed as the percentage of all (ungated) cells in the culture. Each point represents the mean of duplicate determinations. Bars indicate 90% confidence intervals. (o) Cell counts in ADV- and mock-infected cultures. Each point represents the mean of triplicate determinations. Bars indicate 90% confidence intervals. Cell viabilities, judged by trypan blue exclusion, were similar in ADV- and mock-infected cultures (>90% at 0 h and 80 to 90% at 74 h). The lower cell count in ADV-infected cultures at 26 h was due to ADV-induced inhibition of cytokinesis (see text for discussion).

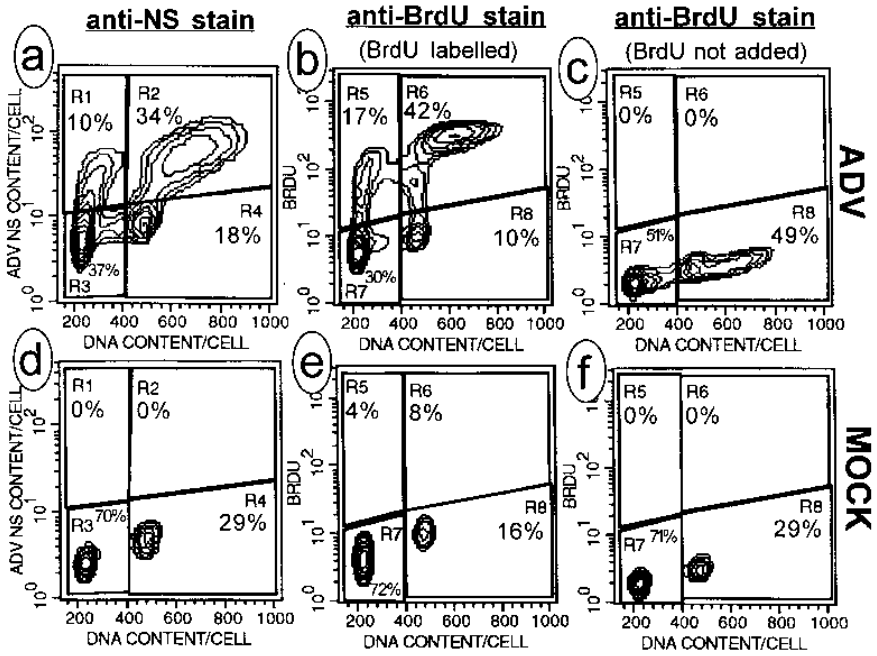

FIG. 5. DNA synthesis in population A and B cells. Synchronized cultures were infected with ADV at 10 FFU/cell or mock infected. BrdU (10 μM) was added at 18 h after release from the HU block (a, b, d, and e), and all cultures were harvested at 20 h. Parallel cultures were double stained for NS proteins and DNA (a and d) or BrdU and DNA (b, c, e, and f) and analyzed by flow cytometry. Contours show 65% differences in cell number (logarithmic spacing) after a 1.5% (a and d) or 3% (b, c, e, and f) background subtraction. Background subtraction prevents contours from appearing in areas of low cell density but has no effect on the percentage of cells indicated in the regions shown in each plot. Regions in the plots in panels a and d have identical positioning and are set around the following populations: R1, population B of NS^+ cells; R2, population A of NS^+ cells; R3, G_1- and S-phase NS^- cells; R4, G_2/M-phase NS^- cells. Regions in the plots in panels b, c, e, and f have identical positioning and were set to correspond to the regions in the plots in panels a and d.

Following conversion to linear values, FITC fluorescence levels were used to compare BrdU incorporation in population A (Fig. 5b, R6) and population B (Fig. 5b, R5) cells. BrdU incorporation in populations A and B was estimated by dividing the average FITC fluorescence of all cells in R6 or R5, respectively, by the average FITC fluorescence of all cells in R8 or R7, respectively (Fig. 5b) (24). Using this method, we reproducibly found that population A cells incorporated 70 to 100% more BrdU than population B cells (the value was 70% in the experiment with the results shown in Fig. 5), in agreement with the augmented cumulative DNA synthesis observed in population A (see above).

It should be mentioned that when same method was used to compare NS protein levels, we found that population A cells contained slightly more NS proteins than population B cells (20% more [Fig. 5a]). However, the significance of this observation is unclear, as some loss of NS proteins likely occurred during ethanol fixation (see above), and the anti-NS serum reacted with both NS1 and NS2 proteins.

Population A cells support ADV DNA replication and production of infectious virus. ADV DNA replication in synchronized cultures was examined by Southern blotting and [^{3}H]thymidine labelling. Only input single-stranded ADV DNA was detected from 0 to 4.5 h postrelease (Fig. 6a). Monomer replicative-form (RF) ADV DNA (13) was first detected at 6.5 h, or at approximately mid-S phase. From 6.5 to 23 h, the amount of ADV DNAs increased strongly, with single-stranded DNA, monomer RF DNA, and dimer RF DNA all being produced.

[^{3}H]thymidine uptake was similar in ADV- and mock-infected cultures from 0 to 12 h (Fig. 6b). From 16 to 25 h, ADV-infected cultures incorporated two to eight times more [^{3}H]thymidine than did mock-infected cultures (Fig. 6b), in agreement with the $>G_2$/M DNA synthesis observed by flow cytometry (Fig. 2j to l). Densitometric scanning showed that the majority of [^{3}H]thymidine uptake from 18 to 25 h occurred in viral DNA (Fig. 6c). (Of the total [^{3}H]thymidine uptake in genomic and viral DNAs, that in viral DNA accounted for 60% at 18.5 h, 85% at 21 h, and close to 100% at 25 h.) Thus, ADV DNA (Fig. 6c) and the $>G_2$/M DNA observed by flow cytometry (Fig. 2j to l) exhibited coinciding replication kinetics.

Since ADV DNA replication occurred at 12 to 14 h (Fig. 6a and c), when only population A was present (Fig. 2j), we conclude that population A cells supported ADV DNA replication. In addition, we found that elimination of population B by colcemide treatment (discussed below) did not affect [^{3}H]thymidine uptake into viral DNA from 18 to 25 h (not shown). This indicated that the great majority of ADV DNA replication (Fig. 6a and c) occurred in population A, but it did not rule out the presence of ADV DNA replication in population B.

Taken together, the findings described above suggested that the $>G_2$/M DNA observed by flow cytometry in population A (Fig. 2l) could be ADV DNA. ADV DNA was in fact produced in quantities (Fig. 6d) that might be expected to influence the PI fluorescence of cells supporting ADV DNA replication. Levels of genomic DNA replication were consistently not increased in ADV-infected cultures from 14 to 25 h (Fig. 6c), arguing against overreplication of genomic DNA in $>G_2$/M-phase cells.

To confirm permissive ADV replication in population A, we assayed production of infectious ADV in cultures in which formation of population B was inhibited. Since infected cells traversed S, G_2, and M phases to join population B, but traversed only S to join population A (Fig. 2f to k), we used colcemide and VM-26 treatment to inhibit formation of population B. When added immediately after release from the HU

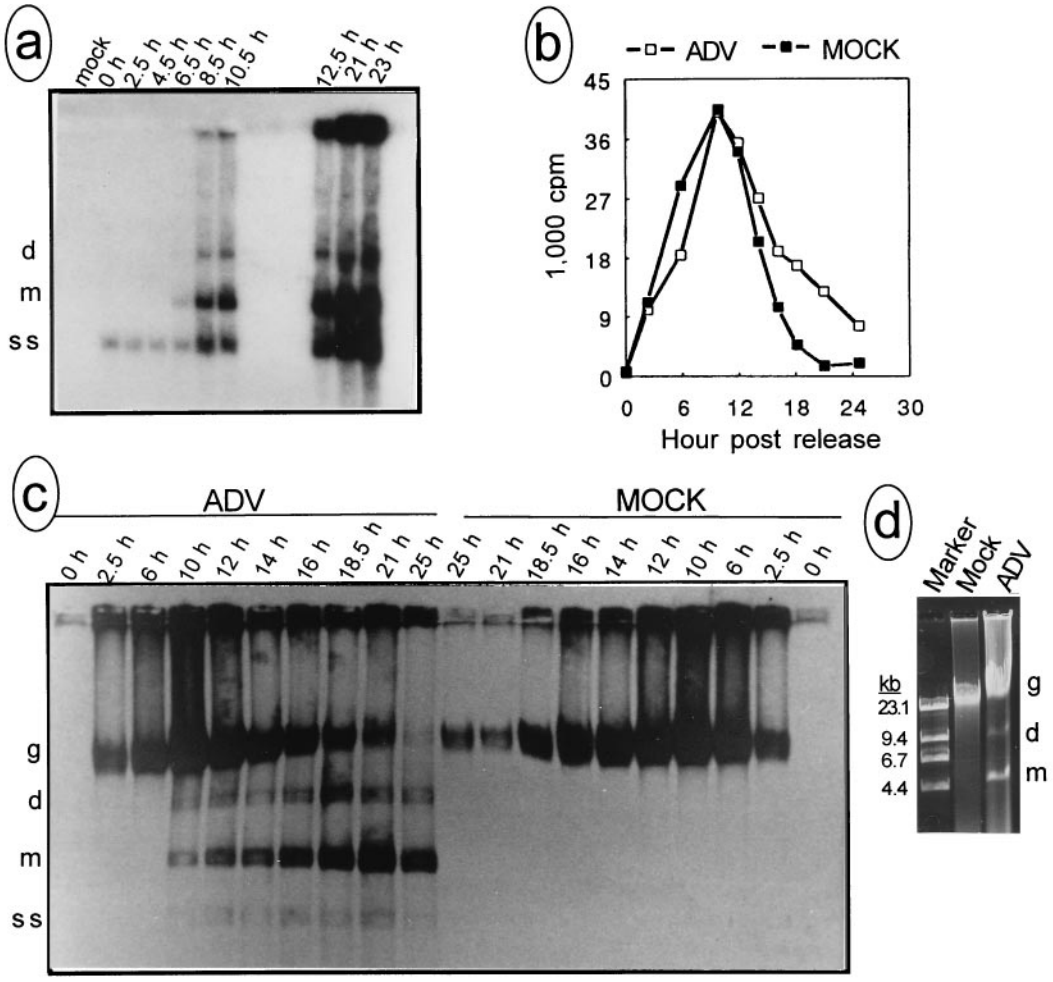

FIG. 6. ADV DNA replication in synchronized cultures. Synchronized cultures were infected with ADV at 10 FFU/cell or mock infected. (a) A Southern blot of total DNA was probed with a ^{32}P-labelled plus-sense ADV riboprobe, which hybridizes to all viral DNA species. ss, single stranded virion DNA; m, monomer RF DNA; d, dimer RF DNA. (b) In a separate experiment, cultures were labelled with 10 μCi of [^{3}H]thymidine per ml for 2 h immediately prior to harvest at the indicated times. HCl-pyrophosphate-precipitable radioactivity incorporated in ADV-infected and mock-infected cultures is shown. (c) Autoradiographic exposure of DNAs from the experiment with the results shown in panel b. Viral DNAs are indicated as in panel a. g, genomic CRFK DNA. (d) Samples from the 25-h time point from the experiment with the results shown in panel b were electrophoresed in 1% agarose and stained with ethidium bromide. The marker was lambda DNA. Densitometric scanning showed that the amount of ADV RF DNA was 10% of the amount of genomic DNA.

block, neither drug prevented S-phase traverse and formation of population A (Fig. 7), although VM-26 did cause a slightly delayed S-phase traverse and delayed $>G_2$/M DNA synthesis in population A (not shown). As expected, both drugs inhibited formation of population B (Fig. 7). Infectious ADV was produced to similar levels in blocked and unblocked cultures (Fig. 8). Since infectious virus was generated in cultures blocked with two differently acting drugs, production occurred in inherently permissive cells and not in drug-induced, nonpermissive cells. More than 90% of infectious virus remained cell associated (Fig. 8), which is characteristic for ADV (14, 36) and makes reinfection unlikely to have contributed to the results. Thus, we conclude that permissive ADV replication, leading to production of infectious ADV, occurred in population A.

DISCUSSION

We report that ADV infection causes a characteristic binary pattern of cell cycle arrest in permissive CRFK cells. ADV-induced cell cycle arrest was S-phase dependent, because normal S-phase traverse was required to trigger production of NS proteins, and the presence of NS proteins was required for cell cycle arrest to occur.

Generally, NS^+ cells exhibited cumulative DNA synthesis, which was apparent by increased PI fluorescence levels over time, as well as uptake of BrdU. This suggests that the ADV-induced cell cycle arrest was not a result of unspecific cellular damage. Instead, ADV apparently interrupted only some cellular functions, while leaving the cellular DNA synthesis machinery, which the virus requires for replication of its own genome, intact.

The majority (55 to 70%) of NS^+ cells were present in a population termed population A. Population A was recruited mostly from cells in later parts of S phase, and formation of population A was not inhibited by VM-26. Thus, population A cells were arrested in late S or G_2 phase.

Population A cells accumulated $>G_2$/M levels of DNA during the ADV-induced late S/G_2 arrest. [^{3}H]thymidine labelling and Southern blot analysis showed that ADV DNA replication occurred in population A and that ADV DNA replication

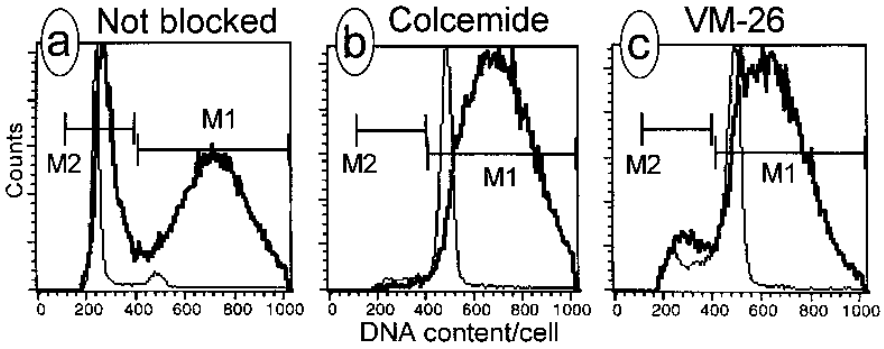

FIG. 7. Elimination of population B by drug treatment. Synchronized cultures were infected with ADV at 10 FFU/cell. At release from the HU block (0 h), cultures were treated with colcemide or VM-26 or left untreated. All cultures were harvested at 25 h. Cells were double stained for ADV NS proteins and total DNA content and analyzed by flow cytometry. NS^+ (thick lines) and NS^- (thin lines) cells were gated as shown in Fig. 4. Markers M1 and M2 indicate the positions of populations A and B of NS^+ cells, respectively.

became dominant in infected cultures at the times when $>G_2$/M DNA synthesis was apparent in population A. This suggests that the $>G_2$/M DNA observed by flow cytometry is ADV DNA. If the $>G_2$/M DNA is viral and PI is assumed to stain predominantly double-stranded viral DNA, flow cytometric measurement of absolute DNA contents (with chicken erythrocyte nuclei as a reference particle [51]) indicates that population A cells contained, on average, the equivalent of 10^6 copies of monomeric (4.8-kb) ADV RF DNA (not shown). Previous studies utilizing radioactive in situ hybridization have shown that cells supporting permissive ADV replication may contain approximately 10^5 copies of ADV RF DNA and 10^5 copies of single-stranded virion DNA (2, 5, 6, 9, 12). Given the great difference in methodologies, as well as the uncertainity about the ability of PI to stain viral single-stranded DNA, the assumption that the $>G_2$/M DNA is exclusively viral is in reasonable agreement with previous estimates of ADV DNA copy numbers. However, whereas we have consistently failed to detect overreplication of genomic DNA in ADV-infected cultures, this possibility cannot completely be ruled out by the [^{3}H]thymidine technique utilized in this study.

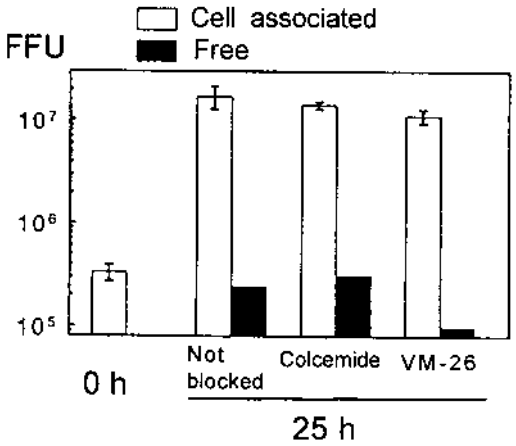

FIG. 8. Production of infectious ADV in synchronized cultures. Synchronized cultures were infected with ADV at 10 FFU/cell. At release from the HU block (0 h), cultures were treated with colcemide or VM-26 or left untreated. Cultures were harvested by scraping at 0 and 25 h, and the content of infectious ADV was determined. The amount of cell-associated virus is shown as the mean of triplicate determinations. Error bars indicate 90% confidence intervals (calculated by using Student's *t* distribution). Free virus in the supernatant was determined for single cultures.

Infection with the autonomous parvovirus minute virus of mice (MVM) inhibits genomic DNA replication (25), and MVM NS1 inhibits heterologous DNA replication (49). By virtue of the relatively late appearance of ADV NS proteins in many S-phase cells, as well as the low percentage of NS^+ cells, putative inhibition of genomic DNA replication by ADV would be expected to cause only minimal reduction in overall genomic DNA replication in ADV-infected cultures. In fact, we did not observe reproducible reductions in genomic DNA replication in ADV-infected cultures, beyond what could be attributed to variability in [^{3}H]thymidine labelling (Fig. 6c). Therefore, methods more accurate than the crude [^{3}H]thymidine labelling technique used in this study are required to define the precise extent of genomic DNA replication in ADV-infected cells.

A minority (30 to 45%) of NS^+ cells were present in a postmitotic population termed population B. Population B cells exhibited low-level DNA synthesis but were unable to traverse S phase. The nature of the DNA synthesis in population B is not known; it might be viral, cellular, or both. Consequently, we cannot at present discriminate between G_1 and early S arrest in population B.

Our results indicated that whereas NS^+ S-phase cells entered population A, population B cells remained NS^- during S phase and expressed high NS levels immediately postmitosis. This suggested a possible explanation for the segregation of NS^+ cells in two distinct populations, namely, that population B resulted from leakage of cells with subthreshold levels of ADV products through the late S/G_2-phase block. We show that new NS^+ cells continuously appeared throughout later parts of S phase, indicating that viral replication initiated in a stochastic manner in S-phase cells (Fig. 2h to j). Thus, failure to reach critical levels of ADV products, and consequent leakage through the late S/G_2 block and into population B, might result merely from the timing of initiation of ADV replication in S-phase cells.

Flow cytometric measurement of BrdU uptake and PI fluorescence indicated that population A cells accumulated approximately threefold-higher burdens of DNA than population B cells during the ADV-induced cell cycle arrest. Clearly, the type of cell cycle arrest was not trivial but influenced the intracellular milieu. Since parvovirus replication depends heavily on cellular factors, induction of late S/G_2 arrest might offer better conditions for subsequent ADV replication than induction of G_1/early S arrest. Interestingly, major replication of the autonomous parvoviruses H-1 (39), LuIII (44), and

MVM (20) also occurs during late S phase. The possibility that viral replication might differ in the two NS^+ populations, quantitatively or qualitatively, is intriguing. However, precise comparison of viral replication at the cellular level in the two NS^+ populations will require cell sorting.

The antiproliferative effects of parvovirus infection are well known (reviewed in references 40, 42, and 54). Different autonomous parvoviruses cause inhibition of mitosis (44, 50), extended DNA synthesis in infected cultures (20, 35), and increases in the number of DNA-synthesizing cells in infected cultures (25), all of which could result from an S/G_2-phase arrest similar to the one we describe for ADV. The molecular mechanisms by which ADV interrupts the cell cycle remain unknown. However, ADV-induced cell cycle arrest is likely to be at least partly mediated by NS1, because preliminary experiments indicate that CRFK cells transiently transfected with ADV NS1 expression plasmids arrest in late S or G_2 phase (46). Similarly, MVM NS1 causes G_2 arrest (34).

In Aleutian disease, ADV replication occurs in immune system compartments associated with cell proliferation, such as bone marrow and stimulated germinal centers in lymph nodes (5, 6). This suggests that the reciprocal regulatory interactions between ADV replication and cell proliferation described in this study may also occur in vivo. The severe dysregulation of the immune system during Aleutian disease may be due to deranged cytokine release from immune system regulatory cells, notably macrophages (reviewed in reference 12). It has been suggested that ADV may infect macrophages by an antibody-dependent mechanism (30, 31). The formation of population B illustrates a general mechanism by which ADV could target other postmitotic, differentiated effector cells in the immune system without the need for extracellular spread, namely, by leakage of ADV-infected cells from proliferative precursor cell compartments. Regardless of the nature of the target cell, ADV-induced cell cycle arrest might modify the host cell fate following viral infection. Cytotoxic T lymphocytes have been shown to be more efficient in killing cycling targets than in killing noncycling targets (32). Thus, ADV-induced cell cycle arrest could conceivably render infected cells poor targets for cytotoxic T lymphocytes and promote intracellular persistence of ADV. Induction of cell cycle arrest has been linked to viral persistence for other viruses (10, 26, 41). However, further studies are necessary to decide whether ADV-induced cell cycle disturbances have pathogenic significance.

ACKNOWLEDGMENTS

This work was supported by a stipend to M.B.O. from the Royal Veterinary and Agricultural University of Copenhagen and by grants to S.A. from the Danish Agricultural and Veterinary Research Council.

We thank Bent Aasted for an introduction to flow cytometry. Torben Storgård, Birgitte Viuff, Susanne Broll, and Jesper Christensen participated in helpful discussions and provided expert technical support.

REFERENCES

1. **Aasted, B.** 1989. Mink infected with Aleutian disease virus have an elevated level of CD8-positive T-lymphocytes. Vet. Immunol. Immunopathol. **20:**375–385.
2. **Alexandersen, S.** 1990. Pathogenesis of disease caused by Aleutian mink disease parvovirus. Acta Pathol. Microbiol. Immunol. Scand. Sect. A. **98**(Suppl. 14)**:**1–32.
3. **Alexandersen, S., and M. E. Bloom.** 1987. Studies on the sequential development of acute interstitial pneumonia caused by Aleutian disease virus in mink kits. J. Virol. **61:**81–86.
4. **Alexandersen, S., M. E. Bloom, and S. Perryman.** 1988. Detailed transcription map of Aleutian mink disease parvovirus. J. Virol. **62:**3684–3694.
5. **Alexandersen, S., M. E. Bloom, and J. Wolfinbarger.** 1988. Evidence of restricted viral replication in adult mink infected with Aleutian disease of mink parvovirus. J. Virol. **62:**1495–1507.
6. **Alexandersen, S., M. E. Bloom, J. Wolfinbarger, and R. E. Race.** 1987. In situ molecular hybridization for detection of Aleutian mink disease parvovirus DNA by using strand-specific probes: identification of target cells for viral replication in cell cultures and in mink kits with virus-induced interstitial pneumonia. J. Virol. **61:**2407–2419.
7. **Alexandersen, S., S. Larsen, B. Aasted, Å. Uttenthal, M. E. Bloom, and M. Hansen.** 1994. Acute interstitial pneumonia in mink kits inoculated with defined isolates of Aleutian mink disease parvovirus. Vet. Pathol. **31:**216–228.
8. **Alexandersen, S., S. Larsen, A. Cohn, Å. Uttenthal, R. E. Race, B. Aasted, M. Hansen, and M. E. Bloom.** 1989. Passive transfer of antiviral antibodies restricts replication of Aleutian mink disease parvovirus in vivo. J. Virol. **63:**9–17.
9. **Alexandersen, S., T. Storgaard, N. Kamstrup, B. Aasted, and D. D. Porter.** 1994. Pathogenesis of Aleutian mink disease parvovirus infection: effects of suppression of antibody response on viral mRNA levels and on development of acute disease. J. Virol. **68:**738–749.
10. **Bartz, S. R., M. E. Rogel, and M. Emerman.** 1996. Human immunodeficiency virus type 1 cell cycle control: Vpr is cytostatic and mediates G_2 accumulation by a mechanism which differs from DNA damage checkpoint control. J. Virol. **70:**2324–2331.
11. **Bloom, M. E., S. Alexandersen, S. Perryman, D. Lechner, and J. B. Wolfinbarger.** 1988. Nucleotide sequence and genomic organization of Aleutian mink disease parvovirus (ADV): sequence comparisons between a nonpathogenic and a pathogenic strain of ADV. J. Virol. **62:**2903–2915.
12. **Bloom, M. E., H. Kanno, S. Mori, and J. B. Wolfinbarger.** 1994. Aleutian mink disease: puzzles and paradigms. Infect. Agents Dis. **3:**279–301.
13. **Bloom, M. E., L. W. Mayer, and C. F. Garon.** 1983. Characterization of the Aleutian disease virus genome and its intracellular forms. J. Virol. **45:**977–984.
14. **Bloom, M. E., R. E. Race, and J. B. Wolfinbarger.** 1980. Characterization of Aleutian disease virus as a parvovirus. J. Virol. **35:**836–843.
15. **Bloom, M. E., R. E. Race, and J. B. Wolfinbarger.** 1987. Analysis of Aleutian disease of mink parvovirus infection using strand specific hybridization probes. Intervirology **27:**102–111.
16. **Braylan, R.** 1993. Dual parameter DNA and surface markers, p. 98–99. *In* J. P. Robinson (ed.), Handbook of flow cytometry methods. Wiley-Liss, New York, N.Y.
17. **Caillet-Fauquet, P., M. Perros, A. Brandenburger, P. Spegelaere, and J. Rommelaere.** 1990. Programmed killing of human cells by means of an inducible clone of parvoviral genes encoding nonstructural proteins. EMBO J. **9:**2989–2995.
18. **Christensen, J., T. Storgaard, B. Bloch, S. Alexandersen, and B. Aasted.** 1993. Expression of Aleutian mink disease parvovirus proteins in a baculovirus vector system. J. Virol. **67:**229–238.
19. **Christensen, J., T. Storgaard, B. Viuff, B. Aasted, and S. Alexandersen.** 1993. Comparison of promoter activity in Aleutian mink disease parvovirus, minute virus of mice, and canine parvovirus: possible role of weak promoters in the pathogenesis of Aleutian mink disease parvovirus infection. J. Virol. **67:**1877–1886.
20. **Cotmore, S. F., and P. Tattersall.** 1987. The autonomously replicating parvoviruses. Adv. Virus Res. **33:**91–174.
21. **Cotmore, S. F., and P. Tattersall.** 1989. A genome-linked copy of the NS-1 polypeptide is located on the outside of infectious parvovirus particles. J. Virol. **63:**3902–3911.
22. **Cotmore, S. F., and P. Tattersall.** 1995. DNA replication in the autonomous parvoviruses. Semin. Virol. **6:**271–281.
23. **Darzynkiewicz, Z.** 1993. Mammalian cell-cycle analysis, p. 45–68. *In* P. Fantes and R. Brooks (ed.), The cell cycle: a practical approach. Oxford University Press, New York, N.Y.
24. **Dolbeare, F., W. Beisker, M. G. Pallavicini, M. Vanderlaan, and J. W. Gray.** 1985. Cytochemistry for bromodeoxyuridine/DNA analysis: stoichiometry and sensitivity. Cytometry **6:**521–530.
25. **Hardt, N., C. Dinsart, S. Spadari, G. Pedrali-Noy, and J. Rommelaere.** 1983. Interrelation between viral and cellular DNA synthesis in mouse cells infected with the parvovirus minute virus of mice. J. Gen. Virol. **64:**1991–1998.
26. **He, J., S. Choe, R. Walker, P. Marzio, D. O. Morgan, and N. R. Landau.** 1995. Human immunodeficiency virus type 1 viral protein R (Vpr) arrests cells in the G_2 phase of the cell cycle by inhibiting p34cdc2 activity. J. Virol. **69:**6705–6711.
27. **Jensen, P. Ø., J. K. Larsen, I. J. Christensen, and P. E. J. van Erp.** 1994. Discrimination of bromodeoxyuridine labelled and unlabelled mitotic cells in flow cytometric bromodeoxyuridine/DNA analysis. Cytometry **15:**154–161.
28. **Johnson, R. T., C. S. Downes, and R. E. Meyn.** 1993. The synchronization of mammalian cells, p. 1–24. *In* P. Fantes and R. Brooks (ed.), The cell cycle: a practical approach. Oxford University Press, New York, N.Y.
29. **Kaaden, O.-R., E. Bartel, L. Haas, D. Kierek-Jaszczuk, M. Löchelt, F. Muller, R. Neth, S. Roth, B. Stolze, S. van Dawen, G. Voss, and K. Willwand.** 1990. Mechanisms contributing to the virus persistence in Aleutian disease. Dtsch. Tieraertzl. Wochenschr. **97:**96–99.
30. **Kanno, H., J. B. Wolfinbarger, and M. E. Bloom.** 1993. Aleutian mink

disease parvovirus infection of mink macrophages and human macrophage cell line U937: Demonstration of antibody-dependent enhancement of infection. J. Virol. **67:**7017–7024.
31. **Kanno, H., J. B. Wolfinbarger, and M. E. Bloom.** 1993. Aleutian mink disease parvovirus infection of mink peritoneal macrophages and human macrophage cell lines. J. Virol. **67:**2075–2082.
32. **Nishioka, W. K., and R. M. Welsh.** 1994. Susceptibility to cytotoxic T lymphocyte-induced apoptosis is a function of the proliferative status of the target. J. Exp. Med. **179:**769–774.
33. **Oleksiewicz, M. B., F. Costello, M. Huhtanen, J. B. Wolfinbarger, S. Alexandersen, and M. E. Bloom.** 1996. Subcellular localization of Aleutian mink disease parvovirus proteins and DNA during permissive infection of Crandell feline kidney cells. J. Virol. **70:**3242–3247.
34. **Op De Beeck, A., F. Anouja, S. Mousset, J. Rommelaere, and P. Caillet-Fauquet.** 1995. The nonstructural proteins of the autonomous parvovirus minute virus of mice interfere with the cell cycle, inducing accumulation in G2. Cell Growth Differ. **6:**781–787.
35. **Parris, D. S., and R. C. Bates.** 1976. Effect of bovine parvovirus replication on DNA, RNA, and protein synthesis in S phase cells. Virology **73:**72–78.
36. **Porter, D. D., A. E. Larsen, N. A. Cox, H. G. Porter, and S. L. Suffin.** 1977. Isolation of Aleutian disease virus of mink in cell culture. Intervirology **8:**129–144.
37. **Porter, D. D., A. E. Larsen, and H. G. Porter.** 1969. The pathogenesis of Aleutian disease of mink. I. In vivo viral replication and the host antibody response to viral antigen. J. Exp. Med. **130:**575–589.
38. **Race, R. E., B. Chesebro, M. E. Bloom, B. Aasted, and J. Wolfinbarger.** 1986. Monoclonal antibodies against Aleutian disease virus distinguish virus strains and differentiate sites of virus replication from sites of viral antigen sequestration. J. Virol. **57:**285–293.
39. **Rhode, S. L., III.** 1973. Replication process of the parvovirus H-1. I. Kinetics in a parasynchronous cell system. J. Virol. **11:**856–861.
40. **Rommelaere, J., and J. J. Cornelis.** 1991. Antineoplasic activity of parvoviruses. J. Virol. Methods **33:**233–251.
41. **Schang, L. M., A. Hossain, and C. Jones.** 1996. The latency-related gene of bovine herpesvirus 1 encodes a product which inhibits cell cycle progression. J. Virol. **70:**3807–3814.
42. **Schlehofer, J. R.** 1994. The tumor suppressive properties of adeno-associated viruses. Mutat. Res. **305:**303–313.
43. **Schoborg, R. V., and D. J. Pintel.** 1991. Accumulation of MVM gene products is differentially regulated by transcription initiation, RNA processing and protein stability. Virology **181:**22–34.
44. **Siegl, G., and M. Gautschi.** 1973. The multiplication of parvovirus LuIII in a synchronized culture system. I. Optimum conditions for virus replication. Arch. Ges. Virus. Forsch. **40:**105–118.
45. **Storgaard, T., J. Christensen, B. Aasted, and S. Alexandersen.** 1993. *cis*-acting sequences in the Aleutian disease mink parvovirus late promoter important for transcription: comparison with the canine parvovirus and minute virus of mice. J. Virol. **67:**1887–1895.
46. **Storgård, T., M. B. Oleksiewicz, and S. Alexandersen.** 1996. Unpublished data.
47. **Tattersall, P.** 1972. Replication of the parvovirus MVM. I. Dependence of virus multiplication and plaque formation on cell growth. J. Virol. **10:**586–590.
48. **Tattersall, P.** 1978. Susceptibility to minute virus of mice as a function of host-cell differentiation, p. 131–150. *In* D. C. Ward and P. Tattersall (ed.), Replication of mammalian parvoviruses. Cold Spring Harbor Laboratory, Cold Spring Harbor, N.Y.
49. **Tenenbaum, L., F. Dupont, P. Spegelaere, L. Zentilin, P. Norio, M. Giacca, S. Riva, A. Falaschi, and J. Rommelaere.** 1993. Inhibition of heterologous DNA replication by the MVMp nonstructural NS-1 protein: identification of a target sequence. Virology **197:**630–641.
50. **Tennant, R. W.** 1971. Inhibition of mitosis and macromolecular synthesis in rat embryo cells by Kilham rat virus. J. Virol. **8:**402–408.
51. **Tiersch, T. R., R. W. Chandler, S. S. Wachtel, and S. Elias.** 1989. Reference standards for flow cytometry and application in comparative studies of nuclear DNA content. Cytometry **10:**706–710.
52. **Tobey, R. A., N. Oishi, and H. A. Crissman.** 1990. Cell cycle synchronization: reversible induction of G2 synchrony in cultured rodent and human diploid fibroblasts. Proc. Natl. Acad. Sci. USA **87:**5104–5108.
53. **Uttenthal, Å., S. Larsen, E. Lund, M. E. Bloom, T. Storgård, and S. Alexandersen.** 1990. Analysis of experimental mink enteritis virus infection in mink: in situ hybridization, serology, and histopathology. J. Virol. **64:**2768–2779.
54. **Vanacker, J. M., and J. Rommelaere.** 1995. Non-structural proteins of autonomous parvoviruses: from cellular effects to molecular mechanisms. Semin. Virol. **6:**291–297.
55. **Viuff, B., B. Aasted, and S. Alexandersen.** 1994. Role of alveolar type II cells and of surfactant-associated protein C mRNA levels in the pathogenesis of respiratory distress in mink kits infected with Aleutian mink disease parvovirus. J. Virol. **68:**2720–2725.